TÉCNICO LISBOA

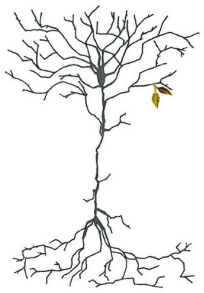

The spatial structure of surround modulation in mouse visual cortex

Beatriz Ferreira Belbut

Thesis to obtain the Master of Science Degree in

Physics Engineering

Supervisor(s): PhD Leopoldo Petreanu and Prof. Bruno Gonçalves

Examination Committee

Chairperson: Prof.
Supervisor: PhD Leopoldo Petreanu
Co-Supervisor: Prof. Bruno Gonçalves
Members of the Committe: Dr.
Prof. Lorem Ipsum

September 2018

We are so familiar with seeing, that it takes a leap of imagination to realize that there are problems to be solved. But consider it. We are given tiny distorted upside-down images in the eyes, and we see separate solid objects in surrounding space. From the patterns of stimulation on the retina we perceive the world of objects and this is nothing short of a miracle.

Acknowledgments

Leopoldo: Biology, hardware, previous software, guidance Tiago Marques: experiments and analysis Gabriela Fiorze: experiments Rhadika: surgeries Oihane: suit2p and surgeries

Rodrigo, Marina, Camille, Hedi discussions, input, environment

Alberto Vale discussion image treatment Bruno Gonçalves connection to Técnico's physics department?

All Champalimaud colleagues and staff: CISS, posters, talks, seminars, knowledge of neuroscience

Abstract

The Objective of this Work ... (English)

Keywords

Keywords (English)

Resumo

O objectivo

Palavras Chave

Palavras-Chave

Contents

List of Figures

List of Tables

Abbreviations

List of Symbols

1

Introduction

Contents

1.1 Motivation

Motivation Section.

1.2 State of The Art

State of The Art Section.

1.2.1 Dummy Subsection A

State of Art Subsection A

1.2.2 Dummy Subsection B

State of Art Subsection B

1.3 Original Contributions

Contributions Section.

1.4 Thesis Outline

Outline Section.

2

Theoretical Introduction

Contents

Present the chapter content.

2.1 Visual Neuroscience: Perception

2.2 Brain visual pathways

2.3 Receptive fields and tuning

2.4 Feedback as a path for contextual information integration

2.5 Surround modulation

2.5.1 Suppression and facilitation

2.5.2 Spatial structure of the phenomenon

2.5.3 The motivation: feedback organization rules - uncovering the functions of feedback

3

Technology

Contents

Developing precise and reliable tools for the spatial and temporal mapping of neuronal activity is crucial to understand the functional architecture of the brain. Radiotracer, electrophisiological, magnetic resonance, anatomic and optical imaging techniques all offer advantages and disadvantages to this end [REFERENCES]. On its part, optical imaging of neuronal activity allows the mapping of large regions of the cortex, varying in time as responses to stimuli. This can be acomplished with voltage sensitive dyes [REFERENCES], changes in the optical properties of the tissue or with the aid of genetic tools. In here, we review the utilized techniques: Intrinsic optical signal imaging that draws on the changing reflectance in the hemodynamics of the cortex and two-photon laser microscopy that takes advantage of genetic manipulation tools.

3.1 Intrinsic signal optical imaging

3.1.1 Acquiring functional maps of neuronal activity

Neuronal activity can comprise the generation and propagation of action potentials, postsynaptic ion fluxes and potentials, neurotransmission, synaptic vesicle recycling, among other processes allocating cerebral cortex energy, along with the maintenance of glial and neuronal resting potentials. Furthermore, the cortex presents activity evoked by sensory stimuli or motor processes, but cortical populations of neurons also show spontaneous coordinated patterns of spiking activity, non-related to any sensory input or motor output.

In regards to the evoked activity, investigating the organizational and functional architecture of the sensory brain requires the means to both detect neuronal activity and to relate these responses to the external stimuli that the subject receives.

The classical approaches developed to this end study animal's brain's *in vivo* by exploring electrophysiological principles: by placing electrodes inside the individual's scalp, one can extracellularly record single cells' electrical activity in a direct manner and access neuron's voltage fluctuations. Multi-unit recordings are also possible through this method.

Other techniques include the 2-deoxy-D-glucose (2DG) autoradiographic method [SOKOLOFF ET AL, 1977] to find and measure glucose consumption in the brain. These metabolic alterations are associated to changes in functional activity and thus an acumulation of the radiolabeled 2DG, representing the integrated rate of glucose consumption, marks the activated areas of the brain.

DYES...

However, many experimental goals require extensive simultaneous recordings while these techniques require long combersome experiments to cover large areas of the cortex. Moreover, electrophysiological mapping methods introduce considerable sampling bias in the recordings as well as poor spacial resolution ($1cm$), while 2-DG maps can only be analysed *post-mortem*, allowing only one experimental session per animal, and can only label two stimulus at the maximum.

Imaging techniques such as functional magnetic resonance imaging (fMRI), near-infrared spectroscopy (NIRS) and intrinsic signal optical imaging (ISOI) introduce less invasive means to simultaneously access larger regions of the brain while the subject is being presented to stimuli and also enable longitudal studies by repeated imaging sessions with the same individual animal. These meth-

ods are based on variations of optically measurable properties of physiological processes associated with neuronal activity.

NIRS....

Intrinsic signal optical imaging (ISOI) enables the visualization of alterations in intrinsic optical properties of neuronal tissues, as a response to neuronal activity.

Slow reflectance light signals are intrinsicly relayed from the surface of the striate cortex due to hemodynamic responses[REFERENCES] that correlate with neuronal activity. Neuronal firing induces blood changes - neurovascular coupling - that produce a light reflectance change.

Neuronal activity requires the hydrolysis of ATP and the oxy-hemoglobin (the protein hemoglobin in red blood cells binded to oxygen) molecules in the capillaries provide the majority of the oxygen used to regenerate ATP via glucose metabolism. Thus, an active brain region is associated with a finely localized increase in oxygen demand and thus a local rise in deoxy-hemoglobin (deoxygenated hemoglobin) and a depletion in oxy-hemoglobin concentrations. This is followed by an hemodynamic response of locally increased blood flow in the capilaries and dilatation of the closeby arteries to replenish and sufice the oxygen requirements.

In this neuronally active situation, the hemodynamic response imposes a light reflectance variation, resulting from three major sources: the changes in blood volume, blood oxygenation and light scattering.

The blood volume component of the signal is the least spatially confined of the three factors, but can nevertheless yield alone functional maps, with the injection of fluorescence dyes into the bloodstream [REFERENCE].

The oxymetry signal is used for instance in fMRI techniques that identify the areas of the brain to which more oxygenated blood is being driven to, relying on how the magnetic properties of more and less oxygenated blood differ. A $1 - 2s$ delayed rise in oxygenation is associated to more active cells and brain usage. However, depending on the magnetic field intensity, this technique can have limited spatial resolution, as it relies on the transition phase that is also associated with the dilatation of arterioles adjoining the original activity sites which can cause signal artifacts.

On the other hand, light scattering changes (REFERENCES) allow for precise temporal and spatial functional mappings of neuronal activity. Higher neuronal activity increases light scattering due to factors like (REFERENCES COHEN 1973). This increase peaks within 2-3 s of the stimulus onset.

With these physiological events optical properties' changes, one can extract the optical signals that correlate with that variance and thus with neuronal activity. Since about 13% of the energy consumption is used for maintenance of the resting state and the greater parcel of the cortical metabolized ATP costs are for action potential propagation (about 47%) [REFERENCES], with the remainder for processes related to synaptic transmission, the intrinsic signal has the major contribution from an oxymetry factor that relates to those inhibitory or subtreshold excitatory input processes.

3.1.2 Intrinsic Signal Optical Imaging: the technique

In the technique used in this work, ISOI, the signal brings about information on the oxy-hemoglobin concentrations during neuronal activity. This method is utilized as one of the best balances in spatial resolution and simultaneous coverage of different brain areas.

Illumination by a stable output source at the red wavelenght level of $540nm$ optimally excites the oxygenated blood flow, while the de-oxygenated blood reflects less light at this wavelength [REFERENCES].

These differentiated properties enable the mapping of the most active, de-oxygenated brain areas at the time of the initial local deoxy-hemoglobin increase, since these regions will reflect less red light than the inactive, amply oxygenated cerebral areas.

ISOI utilizes this principle in brain areas which can be reached by light (around $500\mu m$ maximum). In an animal with a window implantation and illumination of its primary cortex surface, one can record the brain area with a charge-coupled device (CCD) camera to monitor the changes in the reflected light signal from each region of the primary cortex of the subject while this animal is presented to stimuli. In this way, one obtains maps that make correspond the stimulation that the subject receives - visual, somatosensory, auditory [REFERENCES]- to the observed refleted light signal profile at that time interval and in that brain region, whitin some relatively high temporal ($80ms$) and spatial resolutions (in the order of $100\mu m$) [REFERENCES].

For both anesthetized and awake animals, the typical ISOI signal follows a tri-phasic structure: An initial dip, a negative peak at about 4-6s after stimulus onset, and a large rebound [GET REFERENCES].[GET IMAGE]

The signals' information is extracted by calculating differences between the reflectances of the imaged brain area at unstimulated baselines and post stimulation time points. For each stimulus, multiple repetitions are held and the respective signals averaged across the same time points.

Furthermore, in regards to the stimuli dependence of the signal's timecourse, the ISOI signal can be divided into a global stimulus-non-specific response and a local stimulus-specific response that is observed from functionally organized cortical columns[REFERENCE]. This latter component stands as the actual mapping signal.

The properties of the ISOI signal in amplitude and temporal dynamics, as well as of its components, depend on both the stimuli and on the wavelength of the ilumination light that the brain is receiving[REFERENCES].

A green light source at 546 nm is found optimal for obtaining an initial image of the brain surface and its blood vessels. On the other hand, a red light at 630 nm mostly translates changes in blood volume and oxygenation and can thus convey the dynamics of neuronal activity, while the animal is being stimulated.

The figure obtained with the green light can be later overlayed with the mapping image obtained with the red light under stimulation. This overlayed image then relates the neurons' activity specification with the vessels anatomy, serving as a functional map. [GET IMAGES]

Furthermore, [REFERENCE] found that the signal's rise time and time to peak were nearly identi-

cal for both short and long stimulus durations. However, the relaxation time course of the signal does depend on the stimuli duration, which imposes an appropriate inter-stimulus interval and/or aware analysis.

3.2 Calcium indicators and transgenic lines

In the future experimental efforts of this project, there's need for large-scale recordings of neural activity. A myriad of different indicators has been presented in literature and used to divergent extends, being that the suitability of each method to each experimental configuration varies with the priority weights given to factors as the neural events detection fidelity, the specificity of the expressed cell types, and the aimed recording's temporal resolution.

In transgenic mice, given neural processes can be marked and visibly expressed. Genetically encoded indicators of neural activity (GEAIs) are optical indicators that allow for observations that cannot come from electrodes or functional magnetic resonance imaging, accessing neuron's populations' dynamic evolutions over time, within a simultaneous, non-intrusive and less biased observation.

A way of accessing the synaptic excitation occurrence is by means of calcium indicators. Ca^{2+} regulates the fusion of synaptic vesicles: Presynaptic terminals contain voltage-gated Ca^{2+} channels (VGCC) in their membranes and their opening occurs when excited by a presynaptic action potential that results in the influx of Ca^{2+} which triggers neurotransmitter release. This influx also happens as action potentials propagate throughout the neuron. In this way, the calcium entry amplifies the marker of neural activity that is wished to detect, by transforming the transient events in the presynaptic membrane into biochemical more prolonged and more widely localized changes.

However, some limitations restrain the use of this sort of indicators: The temporal precision of the process is limited, as the envolved half-decay times can be long: In different family's of GECIs, a trade-off emerges between the signal's responsiveness' strength and it's temporal accuracy.

In the current project, a suited GECI will be selected from the ultra-sensitive GCaMP6 series [**?**]. GCaMP consists of three main components: circularly permuted green fluorescent protein, cpGFP, the chromophore, that is, the region that determines the colour of the compost; calcium-binding protein calmodulin, CaM, and CaM-interacting M13 peptide. Through mutagenesis of this compound, optimizing for sensitivity, GCaMP6 was selected. Besides its great sensitivity, GCaMP6 indicators allow the reliable detection of individual action potentials, the imaging of large neuron populations and small synaptic compartments, all over long time scales. There are GCaMP6 variants suited for different applications, with several overall brightnesses, rise and decay kinetics and calcium affinity properties.

The expression of this compound could be achieved by viral gene transfer using adeno-associated viruses (AAVs). However, besides introducing some level of invasiveness, this method produces different degrees of expression in neurons accourding to their distance to the infection site as well as a continuing increase of expression over time until possible damage to the cells, limiting the imaging time interval of opportunity. These disadvantages can be obviated by transgenic expression of GECIs. The mice that will serve as subjects in this thesis project were genetically modified as to express GCaMP6 in

most neurons of the cortex under the Thy1 promoter [**?**].

GCaMP6 increases green fluorescence in the presence of calcium. As a released neurotransmitter or an action potential opens a VGCC, entering calcium induces the biding of calmodulin (CaM) to a peptide (RS20, homologous to M13). This causes the repositioning of Arg337 (in the CaM domain) which in turn leads to the protonation (loss of a proton) from the chromophore. As the acid dissociation constant decreases, this conformational change of the chromophore induces an absorbance shift and, upon blue excitation, green emission is increased.

3.3 Two-photon laser scanning microscopy

Neuronal phenomena can be relevant in broad scale ranges, both spatially and temporally. With high resolution, sensitivity, contrast and being able to track events over large cortical ranges, two-photon excitation (2PE) laser scanning microscopy provides a way of accessing fluorescent objects, such as the GCaMP6 expressing neurons, by selectively exciting them and detecting the produced light signal. This technique can furthermore be applied to living or intact tissue, with minimal photodamage (phototoxicity and photobleaching). The probability of detecting a signal photon per excitation event is greater than with previous techniques, especially for imaging deep in scattering tissue.

Two low-energy photons (deep red and near IR) are sent by a focused laser to a fluorophore unit and excite, in combination, the higher-energy electronic transition required for the emission of fluorescent light. 2PE is a nonlinear process, as the absorption rate depends on the squared value of light intensity. This intensity drops quadratically with the distance from the focus. Therefore, if the numerical aperture objective is small enough, this excitation is localized, and the excitation can affect a very small focal volume and produce good 3D contrast and resolution.

Another advantage of 2PE is in its relation with scattering. As photons enter tissue, they scatter and deviate their paths according to inhomogeneities found in the refractive index of the medium, and this reduces the amount of light delivered to the focus and from the fluorescent molecule to the detection apparatus. However, 2PE uses near IR beams that penetrate tissue better than visible waves (as used in one-photon microscopy); the non-linearity of 2PE also contributes to the reduced scattered photons; and finally, since the excitation is localized, all the fluorescence photons coming from the excited molecule, even if scattered, portray useful signal, not being lost and not contributing to background noise.

Typically, a laser is focused on a given target plane and scanned over the sample. When an excitation occurs, it is detected by photodetectors. These responses are then summed over some microseconds and mapped to single pixels of an image.

The lasers used for this method should be powerful enough to compensate for the small two-photon cross-sections and produce sufficient signal levels. Moreover, 2PE efficiency increases as the inverse of pulse duration, and the device should thus be suitable for short light pulses. Mode-locked Ytterbium-doped and Cr:forsterite lasers suffice these requirements for the considered wavelengths.

Objectives are used for the essential focusing of the laser beams. Another important consideration regards the detectors: These should cover large sensitive areas (millimeters), as well as contemplate

good gain, quantum efficiency, and other important thresholds. Photomultiplier tubes (PMTs) are usually applied for this purpose.

4

Technical Implementations

Contents

As the first part of this thesis' work development, I implemented and coded the hardware adaptations and software protocols for the real-time behavioral control and stimulus presentation to be used in the experiments with the open-source arduino-based system Bpod, by adapting the previously used microkernel-based system Bcontrol. This implied the ensurement of a syncronized graphical user interface, the comunication between a governing machine, a microscopy apparatus, a stimuli monitor and a bpod device, within minimal processing time, as well as different states matrices and protocols for each stimulation type - RF mapping, tuning mapping and SM properties investigation. Moreover, the system also required proper functionality within the software controling the two-photon microscope, which was enabled by proper understanding of the trigger and configuration requirements of the software ScanImage.

4.1 System's scheme

The experimental procedure of visual stimuli display involved four main components in communication of parameters, configurations and triggered synchronization: A governing machine and a stimulus display matlab instances, a Bpod device and the set of two-photon laser microscopy appliances and software.

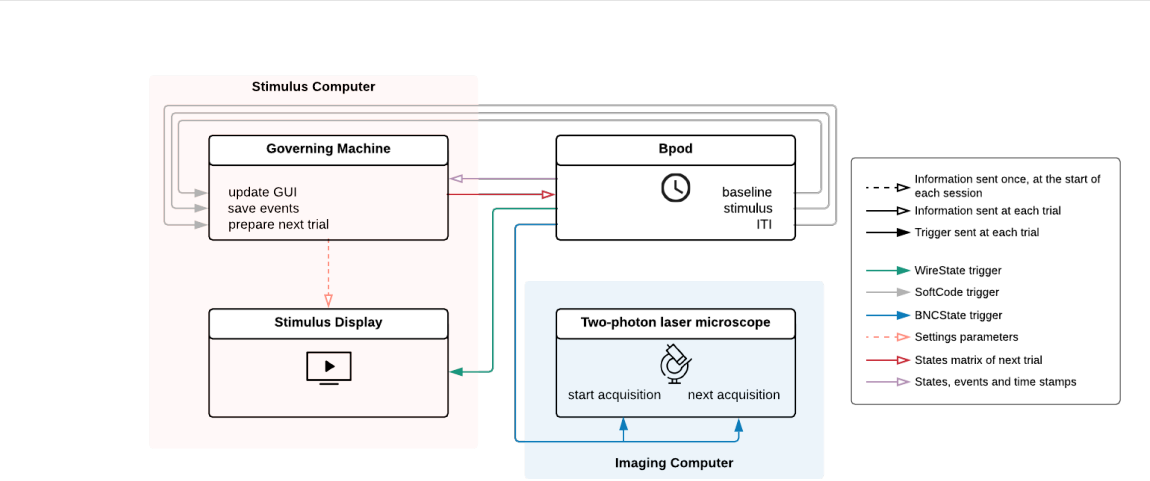

Figure 4.1: Setup and connections scheme of devices used for stimuli presentation and real-time imaging.

Controlled by one of the computers, called here stimulus computer, were the governing machine and the stimulus display.

The governing machine held the Graphical User Interface (GUI) as well as all of the computations and running protocols with Bpod's software for saving the stimuli settings and preparing the stimuli configurations and states matrices for the different trials.

The stimulus display was produced in a second monitor connected to this stimulus computer and operated within a second matlab instance of routines coded with Psychtoolbox software for interfacing between Matlab and the computer screen. This Matlab instance loaded, at the beginning of the session, all of the stimuli settings that were saved in the bpod's Matlab instance. With a counter, the script iterated the full trials structure, displaying the applicable stimuli at the proper times. This timing

synchronization was enabled by triggers received in a NI-DAQ data acquisition board.

The bpod apparatus produced these triggers, connected to the system and taking advantage of a precise internal clock. Having received each trial's state-matrix specifications from the governing machine with enough buffer time, bpod produced the appropriately timed states - the main ones being the baseline, the stimulus and the ITI - and sent the required triggers at each stage. At each trial, in the beginning of the baseline period, a trigger was sent to the governing machine to update the GUI to show the current trial stimuli specifications; during the stimulus presentation, another trigger was sent to save the events of the previous trial and during the ITI an instruction was sent for the governing machine to prepare the next trial by computing the next states matrix with the new trial's stimuli configurations. Bpod also sent, at the beginning of the stimulus display state, the trigger for the stimulus computer second matlab instance to display the loaded and prepared stimulus in the screen visualized by the animal. Finally, at the beginning of the baseline and in the end of the ITI of the proper trials, a trigger was sent to the called imaging computer that held the software controlling the two-photon laser microscope for respectively starting and afterwards completing and proceeding to the next brain scanning acquisition.

The two-photon laser microscope held different components: The laser apparatus with the mirrors, lenses, beam-splitter and remaining light path enforcers; the objective enabling both a bright field and a two-photon configurations; the synchronization device BLACK BOX[?], a NI-DAQ data acquisition board for receiving Bpod's triggers, and finally the imaging computer that operated the controlling software application ScanImage 4 for laser scanning microscopy. This was also the computer that saved the raw image sets acquired from the two-photon scannings at each protocol session.

The sent information and triggers used the different physical wiring possibilities: Firstly, SoftCodes were sent from bpod to the governing machine's computer, via the USB port that connected these devices. From bpod to the stimulus display NI-DAQ board, WireStates were used, and, to the two-photon NI-DAQ board, BNCState triggers were sent. On the other hand, the information about states, events and trial time stamps was sent at each trial via USB from the Bpod device to the bpod's governing machine matlab instance and then saved with its own software. From the governing machine, information was sent as the following trial's state matrix, to the bpod device also via USB and the next trial's settings were sent to the stimulus display matlab instance by saving them at the beggining of each protocol session in a file that was then loaded in the stimulus display matlab before starting the session.

4.2 Software: Governing machine protocols and stimulus presentation

4.2.1 Retinotopy mapping

4.2.2 Implementation and hardware alterations

4.2.3 Surround modulation spatial structure

4.2.4 Stimulus presentation with psychtoolbox

4.2.5 Optical imaging with Scanimage interface

4.3 Hardware: Trigger wiring and two-photon microscopy

4.3.1 Triggering

4.3.2 Two-photon laser microscopy

4.4 Instrumentation

5

Experimental Methods

Contents

Over the experimental process, the appropriate settings of both the animals' state of alertness and of the visual stimulation were chosen as an operative practical balance. In this chapter we describe the methods and specifications of the animals' care and craniotomy cirurgies, as well as the settings of the ISOI and visual stimulation sessions.

5.1 Animals

All procedures were approved by the Champalimaud Centre for the Unknown Ethics Committee and carried under the stipulations of the Portuguese Direção Geral de Veterinária. Mice were held in individual cages on a reversed light-dark cycle with access to food and water. Mice were exclusively used for the experiments regarding this thesis' work.

Cells' somata in V1 layer 2/3 of four Thy1-GCaMP6s ?? male?? mice (?? Laboratory stock no:??) were imaged.

Prior to the imaging experiments, once adults (?? to ?? weaks old), the mice underwent chronic window implantation surgeries. A circular craniotomy of diameter $4mm$ was performed over each mouse's left visual cortex, leaving the dura intact. The imaging windows were constructed using two layers of microscope cover glass (Fisher Scientific, no. 1 and no. 2) and UV-curable optical glue. A window was placed into the craniotomy using black dental cement and an iron headpost was attached to the skull with dental acrylic. The subjects were kept under isoflurane anesthesia, as well as Bupivacaine (0.05%; injected under the scalp) and Dolorex ($1mg/kg$; injected subcutaneously), serving respectively as local and general analgesia. Eye moisturing was insured with ophtalmic ointment (Clorocil, Laboratorio Edol).

For both the ISOI and visual stimuli protocols, the animals were lightly anesthetized with isoflurane (1%) and injected intramuscularly with chlorprothixene (1mg/kg), a muscular paralyzer to circumvert the need for higher anesthesia concentrations which could depress the recorded neuronal responses. Mice were headfixed by the headposts during all of the visual stimuli presentations and their eyes were protected and kept moist with silicone oil (Sigma-Aldrich) in thin, uniformly coated layers.

5.2 Visual stimulation

For both the ISOI and visual stimuli protocols, an LED display (BenQ XL2411Z, 144-Hz monitor, stimulus presented at $60Hz$) was used. The screen was placed at $15cm$ from the mouse's right eye and aligned at 30^o to the axis of its nose-line, insuring access to the visual space of 120^o in azimuth and 60^o in elevation???. The stimuli were produced and presented using Matlab and the Psychophysics Toolbox [REFERENCES] (chapter 3,??).

5.3 Intrinsic signal optical imaging settings

The course of action with each craniotomized mouse started with the performance of intrinsic signal optical imaging (ISOI) over the mice's primary visual cortex and surrounding visual areas [REFERENCES] to obtain a reasonable spatial resolution retinotopic mapping of the temporaly dependent

hemodynamics of the accessed brain while moving visual stimuli was presented to the animal on a monitor aligned to the center of the mouse's right eye and forming a 30^o angle with the animal's nose-line.

The stimuli consisted of a checkerboard of alternate flickering light/dark squares ($5Hz$) that was masked to continuously expose only a periodic drifting stripe of the grid in four consecutive cardinal directions ($12s$ period, 20^o width, 80 times for each direction) - an horizontal stripe going from the top to the bottom of the screen, vice-versa, a vertical stripe going from its left to its right or in the opposite direction.[GET IMAGE]

The cortical surface of an head-fixed mouse was illuminated with a $620nm$ red LED to allow the intrinsic hemodynamic signals to be recorded as optical images of reflectance change correspondent to cortical activity. This recording was held using a Retiga QIClick camera (QImaging) controlled with Ephus[REFERENCE] with a high magnification zoom lens (Thorlabs) at $5Hz$ focused under the cranial window, at the brain surface. A $535nm$ green LED was also used to obtain an image of the cortical vasculature.

For each animal, this resulted in a retinotopical map of 512×512 pixels, representing ??×?? of cortical area. This corresponded to the color-map of cortical encoding of both azimuth and elevation stimuli locations, superimposed on the image of the mouse's vasculature[GET IMAGE]. These correspondence figures were subsequently used as a first-approach guide to encountering the V1 positions aimed for imaging - those whose neurons responded to stimuli in the center of the mouse's visual field where the central stimuli were displayed during the following two-photon microscopy imaging sessions.

5.4 Session and trial structure

The experimental process of a session comprised three main protocols for each mouse and each of that animal's V1 imaged position: A protocol to establish the receptive fields of the imaged neurons (`StimPresProt_RF`), another to regard their tuning properties (`StimPresProt_tuning`) and a last protocol designed for the actual surround modulation examinations (`StimPresProt_RF`).

Each protocol involved a pseudorandomized sequence of trials - N repetitions of X trial types. Repetitions of each stimulus type are required in order to enhance the signal to noise ratio of the responses by trial averaging.

In general, each trial was formed by an initial baseline, a stimulus presentation, and an inter-trial interval (ITI). In both the baseline and the ITI the screen was left at background brightness and contrast level (grey) and its duration was used as buffer time for internal computations and to ensure sufficient Calcium decay from the previous stimulation (from the previous trial in the case of the baseline, and from the same trial in the case of the ITI). A session's total stimuli display duration should not be longer than two hours, as the anesthesia produces cumulative effects in the central nervous system and can start depressing the neuronal responses, impeaching the subsequent study of its relation with the visual stimulation [REFERENCES]. Thus, the durations of these intervals depended on the specific protocol (chapter 4, section d), as a balance between how important was the separation of responses in between trials - the more precise the intended separation, the larger should be the baseline and ITI

durations - and how many trial types and trial repetitions were intended - the more trials, the less duration the baseline and ITI should have.

	Number of trial types	Number of repetitions	baseline (ms)	stimulus (ms)	ITI (ms)
RF	80	14	0	880	120
tuning	32	25	5	900	95
SM	124	15-20	500	1000	500

Table 5.1: Protocol configurations regarding session extension and trial durations.

5.5 Specifics of the protocol settings and visual stimuli

In a session, the three stimuli presentation protocols were ordered as RF mapping, tuning mapping and then the actual SM examination. Each protocol is associated with different stimuli characteristics, specific to the controls or information that were to be required from the final extracted data. Furthermore, each kind of protocol had also distinct specifications in regards to the time durations in the trial structure of the session. The mice were always placed with their right eye parallel and at $15cm$ from the center of the monitor. All of the stimuli measurements will thus follow indicated in degrees at the mice's perspective to the screen, in azimuth (horizontal axis) and in elevation (vertical axis) coordinates. In addition, to compensate for the screen's flatness, spherical corrections were applied to the displayed stimuli, so that what the mice visualized corresponded to the same size of stimuli at each patch location, irrespective of its distance in the screen and that no distortions in the gratings were perceived by the animal. Every protocol underwent pseudorandomization of the trials: Each type of trial appeared the same number of N repetitions, but at shuffled order. The reason for this was to minimize the neurons adaptation [REFERENCES] to the specific trial types, as they had to be repeated a reasonable amount of times for significant analysis.

5.5.1 Receptive Field mapping stimuli

This protocol consisted on the presentation of a 10^o squared cell (in the mouse's referential) with a small moving bar inside. At each trial, this bar moved in four directions, in sequence but at random order - bottom to top (labelled 0^o), left to right (90^o) and the opposite ones (180^o and 270^o, respectively). The moving bar had 4^o width and $25^o/s$ speed, with the dark at $0WHAT$, the light at $204WHAT$ and the background at $102WHAT$. This patch appeared in any of 80 positions in the monitor, which was divided in a 10×10 grid, tiling a circle with 50^o maximum radius from the center. The presentation was repeated in each grid position 14 times, to a total of 1120 trials, at shuffled order whithin each repetition.

At each trial of $1s$, the stimulus played for $220ms$ and was followed by an $880ms$ ITI, summing 19 minutes of RF mapping at each session.

[GET IMAGE]

Feature	Value
cell size (º)	10
cell grid (º)	[10, 10]
maximum radius (º)	50
stim directions (º)	[0 90 180 270]
bar width (º)	4
bar speed (º/s)	10
dark, stim, background light	[0 204 102]

Table 5.2: Configurations regarding the RF mapping protocol stimuli properties.

5.5.2 Tunings mapping stimuli

The selectivity of each neuron was also controlled for spatial and temporal frequencies, as well as for more gratings' directions of movement.

With the same contrast configurations as for the previous protocol, a circular centered patch of 30º was presented at any of 8 directions: the previous and the intermediatedly oriented ones (0º, 45º, 90º, 135º, 180º, 225º, 270º and 315º). The gratings could have 0.02/º or 0.04/º of spatial frequency and $0.5Hz$ or $1Hz$ as temporal frequency. Together, each of these 32 configurations of direction and frequencies were presented in 25 repetitions, totaled at 800 trials and shuffled within the full protocol.

Each trial had $1s$, divided in a baseline of $5ms$, a stimulus presentation of $900ms$ and an ITI of $95ms$, to a total of 14 minutes per session.

Feature	Value
stimulus size (º)	30
stimulus center (º)	[0, 0]
stim directions (º)	[0 45 90 135 180 225 270 315]
spatial frequency (/º)	[0.02 0.04]
temporal frequency (Hz)	[0.5 1]
dark, stim, background light	[0 204 102]

Table 5.3: Configurations regarding the tuning mapping protocol stimuli properties.

5.5.3 Surround Modulation stimuli

Finally, for the SM protocol the frequencies of 0.04/º and $1s$ were chosen based on previous reports of largest V1 stimulation [REFERENCES]. The light contrasts of the gratings went from 0 at dark to 122.5 at background and 255 at the lightest. Each trial had $2s$, with $0.5s$ of baseline, $1s$ of stimuli display and $0.5s$ of ITI.

There were 124 possible trial types, repeated 20 times, to a total of 2480 trials in an 1 hour and 23 minutes session.

Feature	Value
spatial frequency (/º)	0.04
temporal frequency (Hz)	1
central radius (º)	15
surround inner and outer radius (º)	[27 50]
stim directions (º)	[0 90 180 270]
dark, stim, background light	[0 255 122.5]
groups of stimuli	C, S1, S1+C, S2, S2+C

Table 5.4: Configurations regarding the SM protocol stimuli properties.

There were 5 possible patches: a central one and four surround patches in the cardinal positions. The central patch was a circle of 15º radius, as the others were limited by an external circumference of

50º, an inner circumference of 27º (to obtain a 12º gap between the center and the surround patches) and the curresponding bissectors of the screen. For any patch, there were 4 available directions of gratings movement (0º, 90º, 180º and 270º).

With these patches, five groups of stimuli types were used:

- C - only the center patch, in any of the 4 directions of movement (4 types);

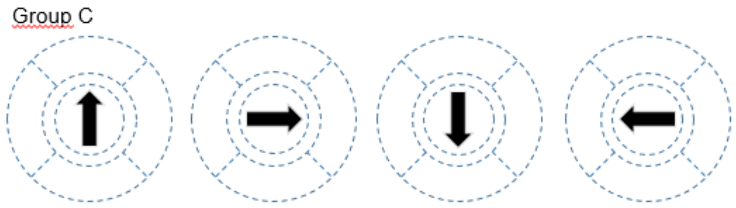

Figure 5.1: Diagram of stimuli group C.

- $S1$ - only one surround patch, in any of the 4 cardinal top, bottom, left or right locations (S1T, S1B, S1L, S1R), and in any of the 4 directions (16 types);

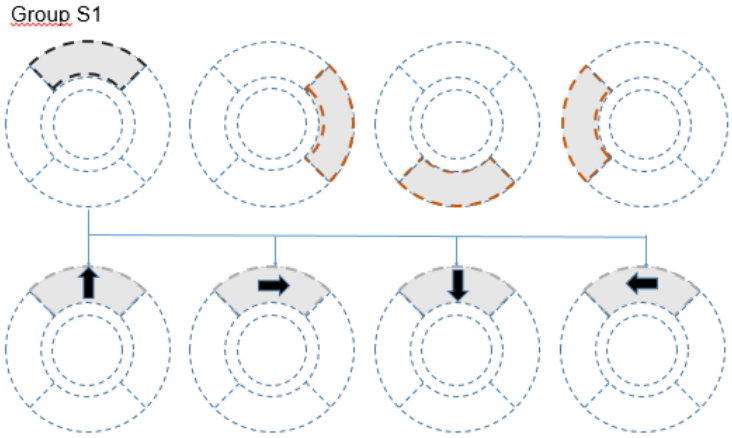

Figure 5.2: Diagram of stimuli group S1.

- $S1 + C$ - One surround patch and the center patch, at any location of the surround($S1T + C$, $S1B + C$, $S1L + C$, $S1R + C$) and any direction for the center and for the surround (64 types);

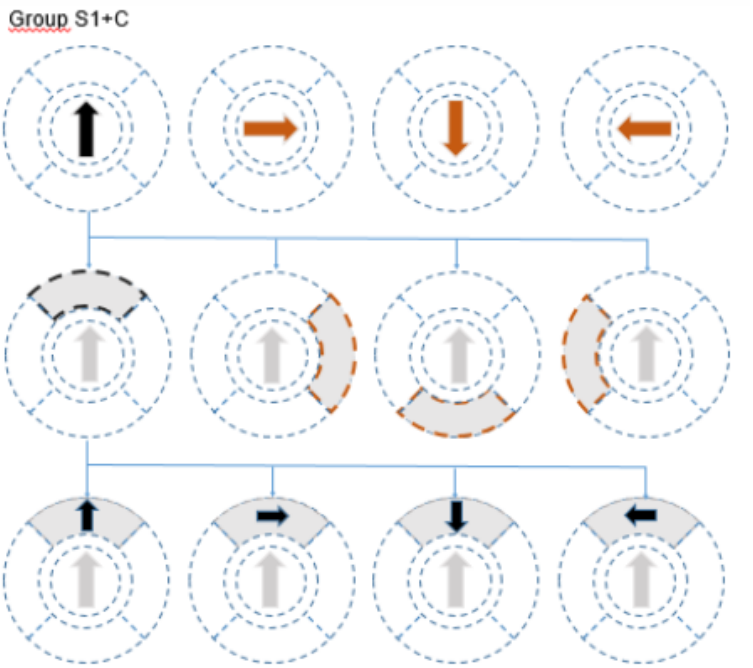

Figure 5.3: Diagram of stimuli group S1C.

- $S2$ - only two surround patches, in opposite cardinal locations, either in the horizontal line ($S2H$) or the vertical line ($S2V$), both of them with gratings moving in the same of any of the 4 directions (8 types);

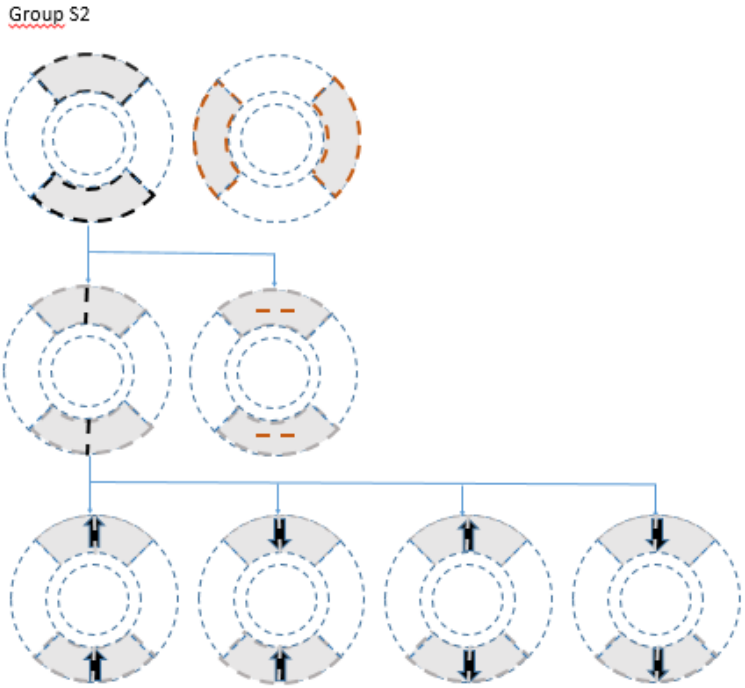

Figure 5.4: Diagram of stimuli group S2.

- $S2 + C$ - Two surround patches and the center patch, both surround patches either in the horizontal ($S2H + C$) or the vertical line ($S2V + C$), both with gratings moving in the same of

the possible directions and the center patch with gratings moving in any direction, not necessarily being the same from the surround stimuli (32 types).

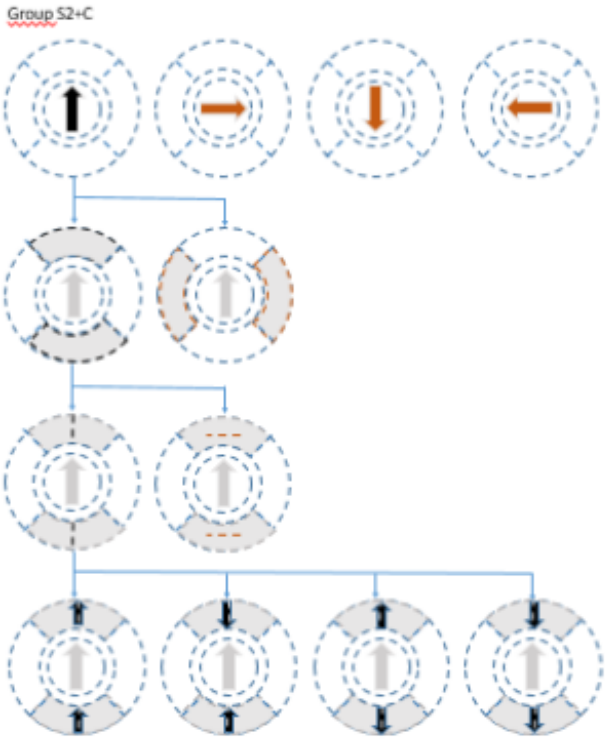

Figure 5.5: Diagram of stimuli group S2C.

Group C was used as a more specific confirmation for the receptive field findings: here the stimuli was now in the center of the screen with the selected size for the analysis. Groups $S1$ and $S2$ provided the data that allowed to exclude from the analysis the cells that responded to stimulation in the defined surround. These had a receptive field that overlapped what we regarded as the surround and thus did not meet the criteria for investigating surround modulation effects in this experiment's designed manner. With the cells that did respond to group C but did not to group $S1$ nor $S2$, we could then regard the effects of actual surround stimulation by examinating the responses to stimuli in the groups $S1 + C$ and $S2 + C$.

6

Analysis

Contents

Present the chapter content.

6.1 Pre-processing images

6.1.1 Cropping

6.1.2 Separating planes

6.2 Suit2p pipeline

6.2.1 Registration

6.2.2 Selection of regions of interest (ROIs)

6.2.3 ROI labelling and quality control

6.2.4 Trace extraction and spike deconvolution

6.3 Data treatement

6.3.1 Receptive field mapping

6.3.2 Tuning mapping

6.3.3 Surround modulation protocol

7

Results

Present the chapter content.

8

Conclusions and Future Work

Conclusions Chapter

A

Title of AppendixA